

Optimization of the Pulsed Electron Avalanche Knife for Anterior Segment Surgery

Daniel Palanker, Alexander Vankov, Kalayaan Bilbao, Michael Marmor, Mark Blumenkranz

Department of Ophthalmology and W.W. Hansen Experimental Physics Laboratory, Stanford University, Stanford, CA 94305-4085

ABSTRACT

Precise and tractionless tools are needed for cutting and ablation of ocular tissue in such operations as vitreoretinal surgery, capsulotomy, non-penetrating trabeculectomy and many others. Previously we reported about the Pulsed Electron Avalanche Knife capable of tractionless dissection of soft tissue in liquid media using the 100 ns-long plasma-mediated electric discharges applied via a 25 μm inlaid disk electrode. In this work we present a next step in the development of this technique, which dramatically improves its precision, the cutting rate and the scope of applicability. (1) Due to spherical geometry of the discharge with the disk-like microelectrode the width of the cut was equal to its depth. To overcome this limitation we apply now a thin cylindrical electrode where the width and the depth of the cut are controlled independently. (2) Cavitation accompanying the sub-microsecond explosive evaporation was a major limiting factor in precision of this technique. In a new modality we apply bursts of pulses, which allow for much higher energy deposition without increase in the size of the transient vapor cavity. (3) Coagulation regime for blood vessels larger than 25 microns in diameter was not possible in the initial approach. It is now available due to extension of the electrode in one dimension. (4) Increase in pulse duration up to several tens of microseconds allows for reduction in voltage and, consequently, in width of the insulator. This, in turn, enables development of the ultra-thin electrodes that can be applied via an intraocular endoscope or 25 G needles.

The new device was found capable of rapidly and precisely dissecting virtually all types of ocular tissue: from soft membranes to cornea and sclera. In addition to vitreoretinal surgery its applications can now expand into anterior chamber surgery including capsulotomy and trabeculectomy.

Keywords:

Plasma-mediated discharge, pulsed electrosurgery, capsulotomy, trabeculectomy, vitreoretinal surgery.

INTRODUCTION

Current mechanical approaches towards vitreo-retinal surgery carry distinct risks including traction tears and imprecise depth of cuts (leading to excessive collateral damage, nicked vessels, etc.). Dielectric breakdown-based dissection of tissue with short-pulsed (0.1 ps to 10 ns durations) lasers[1-3], while helping to reduce traction-related damage and improving cutting precision, is limited in vitreo-retinal applications due to potential damage to the photosensitive retina[1, 4] by light propagating beyond the focal point. In addition, large optical aberrations, for example while operating on peripheral retina, reduce the precision and safety of this procedure. Pulsed shallow-penetrating lasers (Er:YAG and ArF excimer) delivered into the eye via optical fibers[5-7] enable localized treatment of tissue with uniform accuracy at all points in the fundus. However, these instruments have failed to achieve widespread acceptance in vitreo-retinal surgery due to their prohibitively high cost, large size, and relatively slow pace[7, 8].

To address the disadvantages of both mechanical and laser-based instrumentation for tissue dissection in intraocular surgery, we have designed and previously described a device called Pulsed Electron Avalanche Knife (PEAK). This instrument uses high electric field rather than laser photons to create plasma in front of the intraocular probe, and thus it is compact and inexpensive. Overheating of water by the plasma-mediated discharge causes explosive vaporization and rapid expansion of the cavitation bubble (~ 90 m/s) fragmenting the tissue in a proximity to the probe. Previously, we have demonstrated[9, 10] that PEAK is capable of dissection of retinal tissue, as well as epiretinal membranes, lens capsule, and lens cortex. However, extensive testing of this device has revealed the following

limitations: (1) An inlaid disk electrode embedded into insulating probe cannot penetrate into tissue and thus can only produce shallow cuts on its surface. (2) Due to its pulsed regime this device produces a series of perforations in tissue, which not always merge into a continuous cut. (3) Cavitation bubbles accompanying each pulse create collateral damage in tissue which exceeds the size of electrode and corresponding zone of initial energy deposition[11]. Reduction in pulse energy helps to reduce this mechanical damage, but also leads to decreased cutting depth. (4) Small size of the electrode (25 μm) limits the heating zone and does not allow for coagulation of significant blood vessels.

To overcome these limitations we developed a new version of this device using an elongated (penetrating) electrode. Such electrode cuts tissue with its edge rather than just with its apex.

PRINCIPLE OF OPERATION

The principle of this new instrument is based on formation of a thin layer of plasma around microelectrode in a conductive liquid medium using pulsed waveforms that allow for minimization of both, the cavitation- and the heat diffusion-related damage. Strong cavitation can be avoided if energy is delivered using pulses much longer than the bubble formation time (typically sub-microsecond). Efficiency of the energy conversion from the discharge into mechanical energy of the bubble decreases with increasing pulse duration, as shown in Figure 1. To avoid strong effects of electrochemical reactions, such as gas formation, etching of electrode and chemical damage to tissue, the 50% duty cycle charge-balanced burst of pulses was applied instead of a single pulse of similar duration. If the intervals between the pulses do not exceed the lifetime of the vapor cavity the ionization is maintained until the cavity collapses. For example, the lifetime of the 100 micrometer-wide cavity is about 10 microseconds, thus pulses within a burst should be delivered at intervals no longer than 10 microseconds. This condition determines the minimal frequency being about 50 kHz. Pulse frequency in our experiments did not exceed 1MHz.

The width of the heat diffusion zone depends on duration of the burst. Varying it between 0.1 to 100 ms changes the depth of the heated zone between 10 and 300 μm ranging from single cellular layer with no hemostatic effect to complete hemostasis in most of tissues (see Figure 1).

Electric field around the cylindrical electrode is reciprocal to the distance from it, and the density of the Joule heat generated in liquid by the discharge is reciprocal to the square of that distance. Thus thinner electrode allows for more confined energy deposition. Electric field around the cylindrical electrode scales with distance r as following:

$$E = \frac{E_e r_e}{r} \quad (1)$$

Where E_e is electric field on the surface of the electrode, r_e is radius of the electrode. Thus difference in potentials on surface of the electrode and at distance R from the electrode will be:

$$U_e - U_R = \int_R^{r_e} E(r) dr = E_e r_e \ln(R/r_e) \quad (2)$$

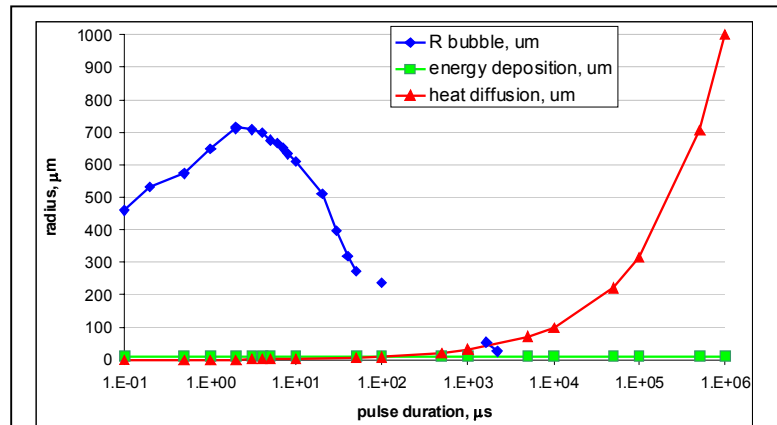


Figure 1. Estimation of the damage zone produced by the pulsed discharge around an electrode of 50 microns in diameter. The blue curve (\blacklozenge) depicts the radius of a single vapor bubble formed by a 1 mJ discharge. At pulse duration above 0.1 ms a series of bubbles is formed with their radii reducing as pulse duration increases (depicted by separate blue dots). The horizontal green line (\blacksquare) represents penetration depth of the electric field (estimated as a radius of the electrode = 25 μm). The red line (\blacktriangle) represents the estimated heat diffusion component assuming a constant temperature of the electrode in one-dimensional (flat) geometry. Optimal pulse duration appears to be between 0.1 and 1 ms, where both the cavitation (blue) and the heat diffusion (red) effects are comparable with the field penetration depth (green).

Electric field becomes spherical at distances larger than the length of the electrode L , thus we can assume that at distances comparable to L the potential drops to zero. Thus

$$E_e = \frac{U_e}{r_e \ln(L/r_e)} \quad (3)$$

Power density of the Joule heat generated in a conductive fluid with resistivity γ is:

$$w = j^2 \gamma = \frac{E^2}{\gamma} = \frac{U_e^2}{r_e^2 (\ln(L/r_e))^2 \gamma} \quad (4)$$

Minimal energy density required for overheating of the surface layer of water

$$A = w \cdot \tau = \rho \cdot C \cdot \Delta T \quad (5)$$

ΔT is the temperature rise in the surface layer of the liquid during the pulse, ρ is density of water, C - its heat capacity. Thus the voltage U required for initiation of vaporization during the pulse duration τ is the following:

$$U = r_e \ln(L/r_e) \sqrt{\rho \cdot C \cdot \Delta T \cdot \gamma / \tau} \quad (6)$$

This voltage and associated with it energy deposition can be reduced by decreasing the radius of the electrode. Assuming the ambient temperature 30°C and boiling temperature 100 °C, $\rho = 1 \text{ g/cm}^3$, $C = 4.2 \text{ J/(g}\cdot\text{K)}$, and $\gamma \approx 70 \text{ Ohm}\cdot\text{cm}$, we obtain $A \approx 300 \text{ J/cm}^3$, and $U \approx 260 \text{ V}$ for $\tau = 0.1 \text{ ms}$, $r = 25 \text{ }\mu\text{m}$, $L = 1 \text{ mm}$.

Similarly to equation (2), the voltage U_{th} required to reach the threshold electric field E_{th} for ionization of the vapor:

$U_{th} = E_{th} r_e \ln(R/r_e)$, where R is the radius of the vapor cavity. Threshold voltage U_{th} can be decreased by reducing the radius of the electrode. This results in a lower power dissipation and consequently in a smaller damage zone in tissue. (7)

CREATING A UNIFORM DISCHARGE IN THE NON-UNIFORM FIELD

Electric field surrounding elongated electrode is very uneven: it is higher in the proximity of the apex and lower in its cylindrical part, as shown in Figure 2. The field enhancement becomes more profound with decreasing diameter of the probe. This non-uniformity leads to the problem that various parts of the probe have very different cutting rate and different damage zone in tissue. Thus outcome of the surgical procedure will strongly depend on which part of the probe was applied. This problem can be avoided by application of the burst of pulses in such a way that vaporization begins first in the areas of highest electric field. Vapor bubble disconnects electrode from the conductive fluid in this zone, while the energy deposition continues in the areas of lower field until it disconnects there, and so on, as shown in Figure 3. In this step-wised fashion a uniform cavity can be created around an electrode with a non-uniform field. Voltage can be selected such that ionization in the cavity occurs only after it is completely isolated from the liquid. This is due to the fact that direct contact of electrode with liquid plays a role of a shunt resistor limiting the voltage across the vapor cavity. A uniform layer of plasma created around a

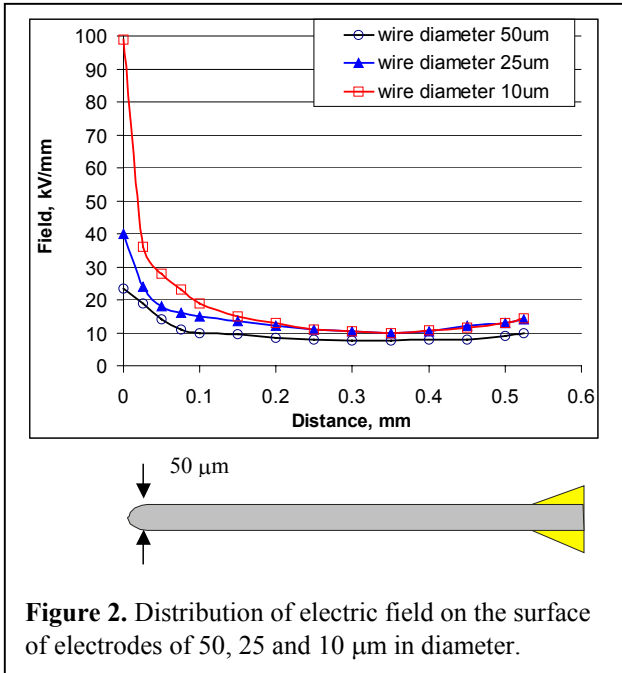


Figure 2. Distribution of electric field on the surface of electrodes of 50, 25 and 10 μm in diameter.

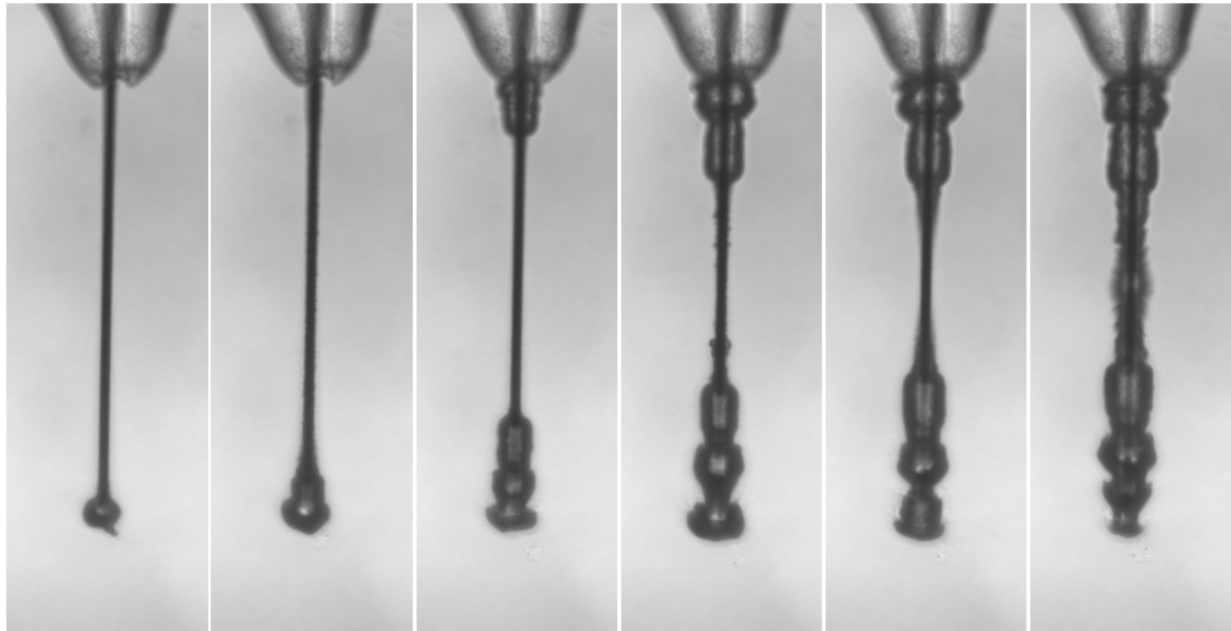


Figure 3. Sequence of photographs illustrating formation of a uniform cavity along the electrode with a non-uniform electric field using a burst of pulses. For complete coverage of the electrode the duration of the burst should not exceed a lifetime of the first bubble. Delays between the beginning of the pulse and the fast flash photograph are: 3, 15, 23, 27, 29 and 30 μ s.

cylindrical electrode is shown in Figure 4.

When tissue is brought into contact with electrode the vapor cavity is thinnest in front of it, and plasma is preferably created in that area, as shown in Figure 5. Thus dissection of tissue preferably occurs in the areas of maximal mechanical resistance.

Strong reduction in size and in expansion velocity of the transient vapor cavity that has been achieved by extension of the pulse duration from 100 ns to 100 μ s eliminated the destructive mechanical effects of the cavitation bubbles. In this regime the leading mechanism of damage became electroporation, i.e. direct effect of electric field on cellular membrane leading to its increased permeability [12]. To minimize this effect the energy is delivered as a burst of pulses of alternating polarity. Measurements on chorioallantoic membranes of chicken embryo using the Propidium Iodide staining [13] demonstrate that damage zone extends to about 50 – 100 microns when electrode of 50 micrometers in diameter is applied at typical surgical settings (pulse duration 100 μ s, energy 2 mJ).

In the regime of the gas-mediated discharge in liquid media the PEAK was found capable of dissecting all types of soft biological tissue: from membranes to cartilage, skin and sclera. Optimal surgical settings were varying for different tissues in the following range: burst duration 100 – 200 μ s, Voltage +/- 450-550 V, frequency 100 – 500 kHz. Typical pulse energy for 50 μ m wire electrode of 0.5 mm in length was about 2.5 mJ. The device was found being very precise and convenient in dissecting the lens capsule. SEM image of the lens capsule cut with a 50 μ m electrode of 250 μ m in length at pulse energy of 1.2 mJ is shown in Figure 6. The edge of the cut is very sharp and clean (compare to the

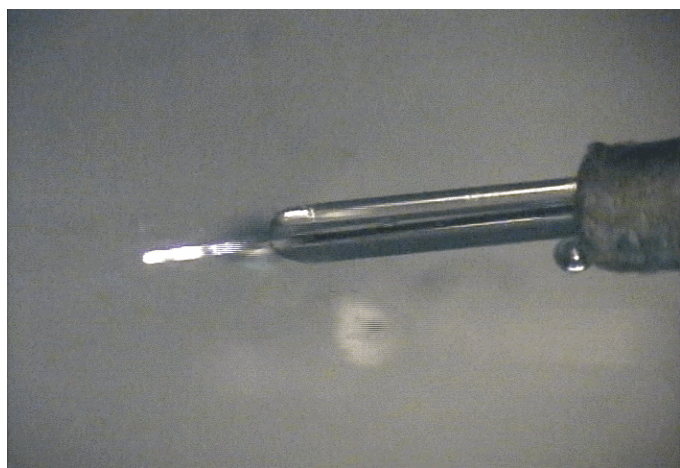


Figure 4. A thin layer of plasma surrounds a cylindrical electrode of 50 μ m in diameter and about 1 mm in length.

scale bar of 10 μm in Figure 6) indicating on low damage associated with dissection in this regime. Tractionless capsulotomy might be very useful for (a) eliminating the risk of peripheral extension of the capsulotomy (radial rips); (b) improving control of the capsulotomy so that it has exactly the desired size; (c) enabling “blind” capsulotomy, i.e. cutting of capsule under the iris in patients with non-dilated pupils; (d) allowing for safe capsulotomy of lens with weak zonules; and (e) allowing for safe capsulotomy when the capsule is difficult to see (e.g. mature white cataracts).

Another interesting application could be a non-penetrating trabeculectomy, where PEAK helps to gain precise control of the post-operative scleral thickness thus reducing the risk of hypotony and anterior chamber leak. It also allows for easier “window” puncture in standard trabeculectomy than a mechanical blade.

Since the size of the heated zone in the steady state is determined by the largest dimension of the source, the maximal width of the coagulation zone is similar to the length of the electrode. That is why thin elongated electrodes, as opposed to the pointed electrodes of the same diameter, are efficient in coagulation.

CONCLUSIONS

PEAK with a gas-mediated discharge on cylindrical electrodes allows for fast cutting of biological tissue without bridges between the two edges. Due to relatively long (tens of microseconds) pulse durations it does not damage tissue by mechanical effects associated with transient vapor bubbles. In this regime PEAK is universally applicable to all types of tissues: from soft membranes to lens capsule, iris and sclera. Collateral damage in this regime is dominated by electroporation and can be limited to a few tens of micrometers. Elongated electrode allows for versatility of shapes (bent probes, loops, etc.), which helps to enhance performance of the device in such applications as vitreoretinal surgery, capsulotomy, irridotomy, non-penetrating trabeculectomy and others.

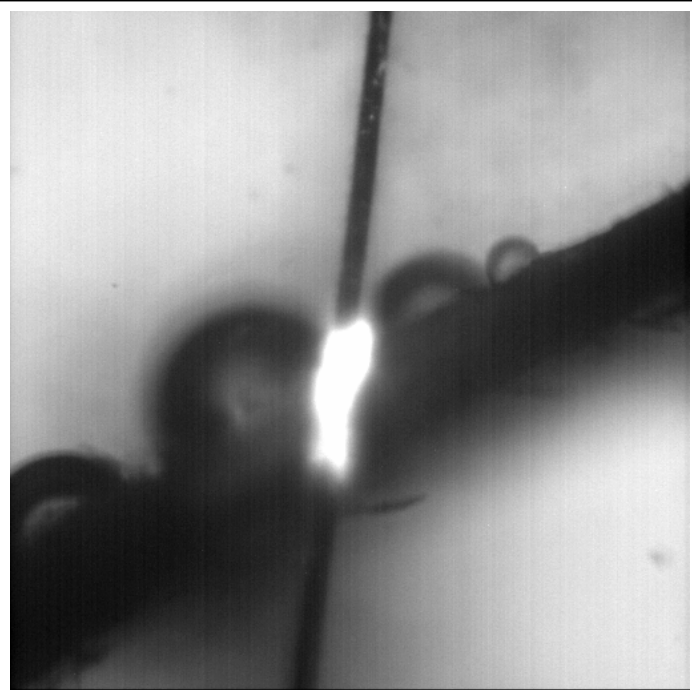


Figure 5. A long electrode of 50 μm in diameter immersed in isotonic saline solution and touching the edge of the paper (dark strip), which is about 250 micron thick. After application of the pulse the plasma is generated only in the area of contact between the electrode and the paper.

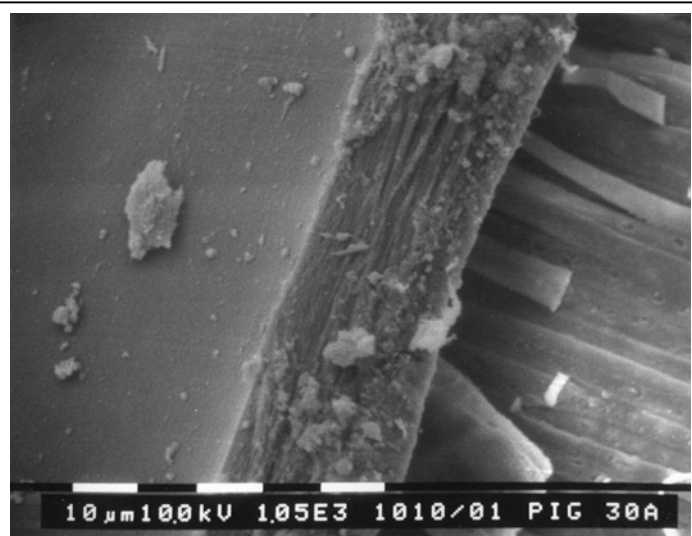


Figure 6. Scanning Electron Micrograph on an edge of the cut produced in the bovine lens capsule by PEAK at pulse energy of 1.2 mJ. Scale bar is 10 μm .

REFERENCES

1. Geerling, G., et al., *Initial clinical experience with the picosecond Nd:YLF laser for intraocular therapeutic applications*. Br J Ophthalmol, 1998. **82**(5): p. 504-9.
2. Lin, C.P., et al., *Intraocular microsurgery with a picosecond Nd:YAG laser*. Lasers Surg Med, 1994. **15**(1): p. 44-53.
3. Vogel, A., et al., *Mechanism of action, scope of the damage and reduction of side effects in intraocular Nd:YAG laser surgery*. Fortschr Ophthalmol, 1990. **87**(6): p. 675-87.
4. Cain, C.P., et al., *Visible lesion thresholds from near-infrared pico and nanosecond laser pulses in the primate eye. Laser-Tissue Interaction VIII, Proc. SPIE*, 1997. **2975**: p. 133-137.
5. Brazitikos, P.D., et al., *Erbium:YAG laser surgery of the vitreous and retina*. Ophthalmology, 1995. **102**(2): p. 278-90.
6. Brazitikos, P.D., et al., *Experimental ocular surgery with a high-repetition-rate erbium:YAG laser*. Investigative Ophthalmology & Visual Science, 1998. **39**(9): p. 1667-75.
7. Hemo, I., et al., *Vitreoretinal surgery assisted by the 193-nm excimer laser*. Invest Ophthalmol Vis Sci, 1997. **38**(9): p. 1825-9.
8. D'Amico, D.J., et al., *Multicenter clinical experience using an erbium:YAG laser for vitreoretinal surgery*. Ophthalmology, 1996. **103**(10): p. 1575-85.
9. Palanker, D.V., et al., *Pulsed electron avalanche knife (PEAK) for intraocular surgery*. Invest Ophthalmol Vis Sci, 2001. **42**(11): p. 2673-8.
10. Palanker, D.V., et al., *Effects of the pulsed electron avalanche knife on retinal tissue*. Arch Ophthalmol, 2002. **120**(5): p. 636-40.
11. Palanker, D., A. Vankov, and J. Miller, *Effect of the probe geometry on dynamics of cavitation*. SPIE, Laser-Tissue Interaction XIII, 2002. **4617**: p. 112-117.
12. Weaver, J.C. and Y.A. Chizmadzhev, *Theory of Electroporation: a Review*. Bioelectrochemistry and Bioenergetics, 1996. **41**(2): p. 135-160.
13. Arndt-Jovin, D.J. and T.M. Jovin, *Fluorescence labeling and microscopy of DNA*. Methods in Cell Biology, 1989. **30**: p. 417-48.